Biogeosciences Discuss., 9, 3071–3098, 2012
www.biogeosciences-discuss.net/9/3071/2012/
doi:10.5194/bgd-9-3071-2012

Biogeosciences Discussions

Novel water source for endolithic life in the hyperarid core of the Atacama Desert

J. Wierzchos[1], A. F. Davila[2], I. M. Sánchez-Almazo[3], M. Hajnos[4], R. Swieboda[5], and C. Ascaso[1]

[1]Museo Nacional de Ciencias Naturales, MNCN-CSIC, Madrid, Spain
[2]NASA Ames Resaerch Center, Moffett Field, USA
[3]Universidad de Granada CIC, Granada, Spain
[4]Institute of Agrophysics PAN, Lublin, Poland
[5]Medical University of Lublin, Lublin, Poland

Received: 29 February 2012 – Accepted: 2 March 2012 – Published: 14 March 2012

Correspondence to: J. Wierzchos (j.wierzchos@mncn.csic.es)

Published by Copernicus Publications on behalf of the European Geosciences Union.

Abstract

The hyperarid core of the Atacama Desert, Chile, is possibly the driest and most abiotic place on Earth, yet endolithic microorganisms thrive inside halite pinnacles that are part of ancient salt flats. The existence of this microbial community in an environment that excludes any other life forms suggests biological adaptation to high salinity and desiccation stress, and indicates an alternative source of water for life other than rainfall, fog or dew. Here we show that halite endoliths obtain liquid water through spontaneous capillary condensation at relative humidity (RH) much lower than the deliquescence RH of NaCl. We describe how this condensation occurs inside nano-pores smaller than 100 nm, in a newly identified halite phase that is intimately associated with the endolithic aggregates. This nano-porous phase helps retain liquid water for long periods of time by preventing its evaporation even in conditions of utmost dryness. Our results explain how life has colonized and adapted to one of the most extreme environments on our planet, expanding the water activity envelope for life on Earth, and broadening the spectrum of possible habitats for life beyond our planet.

1 Introduction

Water is the single most important requirement for life on Earth. While specialized organisms can exist in all but the most arid parts of the Earth, at some point water is too scarce to permit the full range of functions necessary to sustain viable populations of organisms, and biological adaptation to desiccation is no longer possible. We call this threshold the dry limit of life. Understanding the dry limit of life is critical to constrain the water activity envelope for life on Earth, and the possibility of life elsewhere.

There are two known strategies for water acquisition and survival by organisms in extremely dry environments. The first is to colonize substrates where moisture is retained after meager precipitations or snowmelt (Friedmann, 1982), or dew deposition (Büdel et al., 2008; Lange et al., 1994; Kidron, 2000), or fog events (Henschel and Seely,

BGD
9, 3071–3098, 2012

2008; Azúa-Bustos et al., 2011). The underside of translucent quartz, or the interior of porous sandstones are examples of such substrates. A second strategy, exemplified by most lichens and some cyanobacteria, is to supplement liquid water from air humidity (Lange et al., 1994; Palmer and Friedmann, 1990a,b). These strategies have worked successfully in all hot and cold deserts on Earth, except in some parts of the Atacama Desert, in Chile, which appear to be too dry even for these strategies to be effective.

The hyperarid core of the Atacama Desert, located between 20° S and 24° S, receives less than 1 mm yr^{-1} of rainfall (McKay et al., 2003). Soils here are the most abiotic on Earth (Navarro-González et al., 2003), with extremely low concentrations of microorganisms (Navarro-González et al., 2003; Connon et al., 2007; Lester et al., 2007) and trace amounts of degraded, relic organic compounds (Navarro-González et al., 2003; Ewing et al., 2008). The varnish on surface rocks contains scarce quantities of cryptoendolithic bacteria (Kuhlman et al., 2008), whereas epilithic lichens and hypolithic microorganisms, found abundantly outside the hyperarid core (Warren-Rhodes et al., 2006; Wierzchos et al., 2011; Azúa-Bustos et al., 2011), are virtually absent within it (Warren-Rhodes et al., 2006; Wierzchos et al., 2011). This region has been labeled the driest place on Earth and is considered to be close to, or beyond, the dry limit of life.

Surprisingly abundant photosynthetic life has been recently found in the hyperarid core (Wierzchos et al., 2006), inside halite deposits that are part of Neogene salt-encrusted playas, also known as “Salares” (Pueyo et al., 2001). These halite deposits have been isolated from any significant source of surface or ground water for the entire Quaternary, and possibly longer (Pueyo et al., 2001). The halite is shaped in the form of small pinnacles and contains endolithic (rock interior sensu, Golubic et al., 1981; Nienow, 2009) communities of photosynthetic cyanobacteria, along with heterotrophic bacteria and archaea (Wierzchos et al., 2006; de los Ríos et al., 2010). *Chroococcidiopsis*-like cells were the only cyanobacteria found inside the pinnacles, and phylogenetic studies have revealed their closer genetic affinity to *Halothece* genera (de los Ríos et al., 2010). Gene sequences of the heterotrophic bacteria and archaea indicated their proximity to microorganisms found in other hypersaline environments (de los Ríos et al., 2010). The presence of this endolithic community indicates life has found a strategy to survive Atacama's hyper-arid core, where all other colonization strategies have failed.

Davila et al. (2008) showed that water vapor condenses within the halite pinnacles at relative humidity (RH) levels which correspond to the deliquescence point of NaCl (RH = 75 %), and suggested this as a potential water source for the endolithic microorganisms inside the salt. This model implies a close link between the rock substrate and the endolithic communities, and departs from other lithic environments in that the rock substrate itself supplements the liquid water.

However there are still many open questions with regard to this unique endolithic habitat, such as the exact mechanism of water acquisition, the dynamics of liquid water inside the pinnacles, or the interplay between the endolithic communities and the salt substrate. To address these questions, the micro-environmental conditions inside pinnacles were monitored at high temporal resolution for a period of one year. We also conducted non-destructive microscopy investigations to characterize the endolithic habitat from the macro to the micro scale. Our results indicate new mechanisms of water condensation and retention within the halite, and provide further evidence that hygroscopic minerals expand the limits of life in extremely dry environments. The significance of understanding this never before described water source within halite pinnacles from the hyperarid core of the Atacama Desert resides in the fact that it might pushes the dry limit for life outside of the boundaries of our planet.

2 Materials and methods

2.1 Sampling site

The study site was located in the Yungay region of the Atacama Desert (24°05′01″ S; 069°54′52″ W, elevation 969 m), 75 km south-east of the city of Antofagasta, and about

BGD
9, 3071–3098, 2012

60 km from the Pacific Ocean. Yungay receives negligible rain, ($< 1\,mm\,yr^{-1}$, McKay et al., 2003) and the coastal mountains block the marine fog, the so-called "camanchaca", which only reaches the Yungay area in extremely rare occasions. Samples of halite pinnacles were collected for laboratory investigations during a field expedition in January 2010.

2.2 Monitoring of micro-environmental parameters

Microclimate data were collected in situ over a period of one year from January 2010 simultaneously inside and outside a representative halite pinnacles using an Onset HOBO® Weather Station Data Logger (H21-001) connected to a SolarStream® solar-powered transmitter for data transmission by the Iridium Satellite Constellation (Fig. 1a). The array of sensors included photosynthetic active radiation (PAR), temperature (T), relative humidity (RH), electrical conductivity (EC) and a rainfall gauge. Extensive details and images of this set up are provided in the Supplement.

2.3 Mercury intrusion porosimetry

The porosity and pore-size distribution of halite pinnacles were estimated by means of mercury intrusion porosimetry (MIP) (Benavente et al., 2003; Hajnos et al., 2006). MIP was performed on 10 samples for each zone and all data assumed the cylindrical geometry of pores. A micrometrics (Autopore IV 9500) instrument was used to determine connected porosity, pore size distribution and mean pore size in the range of equivalent radii of 0.0015 µm to 173 µm. In the Washburn (or Laplace) equation, a mercury surface tension value of $0.48\,N\,m^{-1}$ and salt-mercury contact angle of 141.3° were used, respectively. Small blocks of NaCl from surface and colonized zones were first air-dried at 20 °C and 20 % of RH for one week and later oven-dried to 105 °C for 24 h and degassed in a vacuum under a pressure of 1.33 Pa at a temperature of 20 °C before analysis. Porosity (total porosity %) was then determined as the weight-normalized volume of mercury intruded in the sample.

BGD

9, 3071–3098, 2012

2.4 Fluorescence microscopy

Fluorescence microscopy (FM) was used to identify and characterize the endolithic communities, and to study the distribution of cells inside the pinnacles. Cross-sections of halite pinnacles were stained with 20 µl of SYBR Green I (SBI) (Molecular Probes), a fluorochrome used for the specific staining of nucleic acid structures of bacteria cells. Bright field images and SYBR Green fluorescence (green signal) and photosynthetic pigments autofluorescence (red signal) were visualized with Zeiss AxioImager D1 fluorescence microscope equipped with Plan-Apo 60x/1.4 Zeiss oil-immersion objective. Specific set of filters: eGFP (Zeiss Filter Set 38; Ex/Em: 450–490/500–550 nm) and for rhodamine (Zeiss Filter Set 20; Ex/Em: 540–552/567–647 nm) respectively was used for green and red signal visualization. Images were recorded with CCD Axiocam HRc (Zeiss) camera and AxioVision 4.7 (Zeiss) software. A detailed description of the FM procedure, as well as applied structural illumination microscopy mode (SIM) can be found in (Wierzchos et al., 2011).

2.5 Low temperature scanning electron microscopy

We used a low temperature scanning electron microscope (LT-SEM) to study the internal structure of colonized halite pinnacles in their natural hydrated state, minimizing sample preparation artifacts. The LT-SEM was equipped with imagining systems using secondary electrons (SE) and backscattered electrons (BSE) detectors, as well as an X-ray energy dispersive spectroscopy (EDS) system. The cryotransfer system of the LT-SEM (CT1500 Cryotrans, Oxford) was composed by shock-freezing stage, cryo-preparation chamber with cold knife, and coating system included a plunge-freezing console, a specimen transfer device, a cryo-preparation unit and a cold stage in the SEM chamber. This set up allowed quenching and stabilizing wet microstructures by ice vitrification (i.e. rapid cooling), transferring and maintaining the sample in cryogenic condition during the whole experiment, cold-knife fracturing of the sample and its surface metal-coating. Block samples (about 10 × 10 × 10 mm) of halite from surface and

BGD
9, 3071–3098, 2012

Novel water source for endolithic life in the hyperarid core of the Atacama Desert

J. Wierzchos et al.

colonized zones were equilibrated for 48 h at different RH levels (20 %, 40 %, 60 %, 70 % or 75 %) using different mixtures of glycerol and water. Then small fragments of halite samples (1 × 1 × 2 mm) were placed in the adjustable slit of the sample holder of the cryotransfer system and fixed to the holder using double-sided adhesive carbon tape. The samples were then plunged frozen in subcooled liquid nitrogen and transferred to the cryo-preparation unit. Next, the frozen specimens were cryo-fractured at −170 °C and etched for 2 min at −90 °C. After ice sublimation from brines by freeze-drying, sample surfaces were gold sputter-coated and then transferred onto the cold stage of the SEM chamber. Fractured and freeze-dried surfaces were observed under a DSM960 Zeiss SEM microscope at −135 °C under conditions of 15 kV acceleration potential, 10 mm working distance and 5–10 nA probe current.

2.6 Environmental scanning electron microscopy

The environmental scanning electron microscope (ESEM) system allows working in the sample chamber during imaging with secondary and backscattered electrons under controlled water vapor pressures and temperature conditions up to water saturation (RH = 100 %). In our experiment, the total pressure in the sample chamber was always equal to the partial pressure of H_2O. Keeping a constant sample temperature at 5 °C and changing the partial H_2O pressure in the range of 0.13 to 8.75 mbar (in steps of 0.13 mbar) during the experiment, allowed us to adjust the RH between 2 % and 100 % inside the ESEM chamber. Small blocks (3 × 3 × 3 mm) of halite were mounted on the stainless steel stub with double-sided carbon adhesive tape. Initially the sample was held for 30 min at low RH (e.g. 20 %) and the RH then increased to the deliquescence RH (DRH) of halite (75 %) in 5 % steps or smaller. After each pressure increase, the sample was inspected for three minutes before the pressure was raised again. During the whole experiment, the secondary electron image was digitalized and stored as single frame and/or as a digital video file to record any morphological changes occurring on the NaCl crystal surface as a function of water vapor pressure. After water film formation was observed at the DRH, the RH inside the ESEM chamber was reduced

BGD
9, 3071–3098, 2012

again to below the point of NaCl crystallization. All observations were conducted in a FEI Quanta 400 instrument.

3 Results and Discussion

3.1 Characterization of endolithic colonization inside halite pinnacles

Generally, halite pinnacles are round-shaped, typically 20–30 cm tall, and appear distributed in a seemingly random fashion (Fig. 1a). Their surface is coated with wind-blown silt and sand particles. Just beneath the surface, there is a non-colonized, light-colored layer approximately 10 mm thick (Fig. 1b), with an average pore radius of 42.65 nm (Table 1). Below that layer there is an inner zone of variable thickness and average pore radius 153.10 nm that contains the endolithic microbial colonies (Fig. 1c,d), with close spatial relations between the different taxa (Fig. 1d). Below this colonized zone there is a non-colonized layer mainly composed of halite and traces of quartz, feldspar, gypsum, glauberite and fine-grained sediment impurities as observed by DRX (not shown).

3.2 Analysis of microclimate data

To address the sources and dynamics of liquid water in the halite pinnacles, we deployed an array of microweather sensors to monitor environmental conditions inside, on the surface and outside the pinnacles at a high temporal resolution for a one-year period (January 2010–January 2011). Open arrow in Fig. 1a shows the location of the microweather station installed among and within the halite pinnacles. Figure 2 shows the variation of monitored micro-environmental parameters, including PAR, T, RH and EC. The rainfall gauge did not record any rain even in the course of one year, and the external PAR, RH and EC sensors did not record fog events, either from low PAR levels, near-saturation RH, or positive EC. Midday clouds where present in two days based on PAR data. The pinnacle surface temperature was monitored using a thermocouple T sensor. Based on this surface temperature measurement and the air RH and air T data, we can also rule out dew condensation on the surface of the pinnacle, based on the Magnus-Tetens formula (Murray, 1967).

Atmospheric RH (blue line in Fig. 2c) never exceeded 75 %, which is the beginning point of halite deliquescence (Davila et al., 2008, 2010; Tang and Munkelwitz, 1993; Ebert, 2002). The maximum RH recorded outside the pinnacles over the year was 74.2 % and mean atmospheric RH was 34.8 % (Table 2). Previous studies in the Yungay region have reported sporadically higher maximum RH values during fog or short rainfall events (McKay et al., 2003; Davila et al., 2008). Despite the absence of liquid water from rainfall precipitation, dew or higher then 75 % atmospheric RH over the course of one year, positive EC signals on the surface and interior of halite pinnacle (Fig. 2d) (i.e. liquid water) and elevated RH values, frequently exceeding 80 % (green line on Fig. 2c), inside the halite pinnacle were observed. Based on those it is possible to differentiate two main stages of moisture conditions within the colonization zone of the pinnacles. The first, or dry stage occurs when atmospheric RH remains below 40 % for several days (blue line in Fig. 3a), and the RH inside the pinnacle is comparably low (green line in Fig. 3a, and values below the pink diamond in Fig. 3b, and Supplement Fig. S2). During the dry stage the surface and interior of the pinnacle are completely dry, as evidenced by the null EC values (Fig. 3a). The second, or wet stage occurs when atmospheric RH exceeds 50–55 % (white diamond on blue line in Fig. 3b), and this is reflected by an EC spike on the surface of the pinnacle (red line in Fig. 3b). If atmospheric RH rises to above 60 %, the spike in surface EC values is followed by high EC values also in the colonized zone (black line in Fig. 3b), indicating liquid water condensation inside the pinnacle. This EC spike in the colonized zone occurs when mean RH inside halite rises above 51.8 % (σ = 9.2; n = 65) (black diamond in Fig. 3b and Supplement Fig. S2). Wet stages always commence during the night or early morning, when air temperature drops and atmospheric RH rises, and can be as short lived as tens of minutes or as long as days or weeks. Remarkably, the longest wet stage, when the EC probe recorded the presence of liquid water (as NaCl brine) inside the halite pinnacle, lasted 40 days (Supplement Fig. S3).

Once the pinnacle interior reached the wet stage, RH values within the pinnacle remained between 75 % and 86.1 % (green lines in Fig. 3b,c), and the conductivity sensor registered its highest values (black lines in Fig. 3b,c), indicating significant amounts of pore-water brine within the colonized zone. It is important to note that during wet stages, conditions inside the pinnacles appeared to be independent of the external conditions (Fig. 3b,c), which frequently remained extremely dry. The wet stage typically terminated when RH inside the pinnacle fell below 41.87 % (σ = 10.8, n = 65) (values below the pink diamond in Fig. 3b and Supplement Fig. S2). At this point the interior of the pinnacle dried up, as reflected by the null EC, and low RH, values.

We note that the occurrences of dry/wet stages were derived from the EC and RH data recorded by the sensors, and therefore represent a first order approximation to the conditions inside the pinnacles. However, our estimates clearly indicate that while conditions outside the pinnacles were always extremely dry, the pinnacle interior remains wet for 5362 h yr^{-1} containing pore water brine available to endolithic microorganisms during 61 % of the year.

Our data shows that halite pinnacles induce the condensation of liquid water at a RH much lower than 75 %, the deliquescence point of halite, and also retain liquid water for up to five weeks, suggesting that liquid water inside halite can occur at much drier conditions and for longer periods of time than previously thought (Davila et al., 2008). This fact points to additional mechanisms of water acquisition and retention in the pinnacles, which are described below. A similar laboratory observation has been described for aqueous sea-salt and NaCl aerosols, which start to absorb water at RH much lower than the DRH and exist as internally mixed phase particles (liquid/solid) over a wide range of RH values (Tang et al., 1997; Koop et al., 2000).

3.3 Internal structure and pore water brine in halite pinnacles

We hypothesize that the tendency of the pinnacles to condense liquid water at a very low RH, and to retain this pore water brine for prolonged periods of time, could be linked to the internal fabric of the pinnacles formed in the characteristic environment of the hyperarid core of the Atacama Desert. To test this theory, we conducted detailed low temperature and environmental scanning electron microscopy observations of the interior of the pinnacles (Figs. 4–7).

A low temperature (or cryo) preparation technique for scanning electron microscopy (LT-SEM) is essential for the observation of a sample in its "natural" hydrated state (Ascaso et al., 2002; Souza-Egipsy et al., 2002). Moreover, visualization of cryo-fixed, cryo-fractured and freeze-dried samples shows the internal structures of the halite features. At the micro-scale, the mineral phase from colonized layer consists of well-defined massive halite crystals, tens of microns in diameter (Figs. 4a,e, and 5a,c). In the pore space between these crystals, we identified a micro and nano-porous phase also composed of NaCl (Figs. 4 and 5). LT-SEM images of cryo-fractured planes in Fig. 4a–c were obtained from halite samples equilibrated at RH = 20 % for 48 h, whereas images in Fig. 4d,e were obtained from halite samples equilibrated at RH = 40 % and 75 %, respectively, for 48 h. At high magnification, this nano-porous phase appears as a cavernous sponge-like structure with capillary-shaped pores as small as a few nanometers (Fig. 4c,d). The nano-porous phase fills the pore space and grain boundaries between massive halite crystals, and contains fully or partially embedded cyanobacterial cells (Fig. 4d,e) and microbial aggregates (Fig. 5a,b). A similar nano-porous phase (as in Fig. 4e) has been experimentally observed (also by LT-SEM) in halite equilibrated with water vapor at RH ≥ 75 % (Desbois et al., 2012, 2008; Schenk et al., 2006). In these studies the nano-porous phase was formed as a sublimated brine remnant after freezing (i.e. from the freezing and sublimation of pore water present in the sample). However, we have also observed the presence of this nano-porous phase inside pinnacles previously oven dried at 60 °C and posterior equilibrated for 48 h at 20 % RH, and at room temperature, when the pinnacles ought to have lost all their water content. As such, we consider that this nano-porous phase was already present in the pinnacles at the time of sampling. The nano-porous phase appears to have a smooth exterior surface (Figs. 4a,b and 5c), and the capillary-shaped pores are only revealed in cryo-fractured plains using LT-SEM. Conventional SEM analyses and visualization with secondary electrons can only show the smooth outer surface, but not the sponge-like texture and capillary-shaped pores. LT-SEM image in Fig. 5a,b shows partially embedded microbial aggregates composed by phototrophic cyanobacteria cells associated by heterotrophic bacteria (arrows in Fig. 5b). LT-SEM observation confirms that all halite pinnacle samples equilibrated at RH $< 75\%$ contained the nano-porous phase.

We applied another in situ visualization approach to further confirm the presence and nature of the nano-porous phase, using the environmental scanning electron microscope (ESEM). The ESEM allows the in situ visualization of samples in their natural state of hydration without any preparation procedure (i.e. without freeze-drying) across a wide and controlled range of RH and temperature values. All ESEM images (Fig. 6) show the nano-porous phase at increasing RH (from 71 % to 77 %) across the deliquescent point of halite, as seen with the backscattered (BSE) detector. As the intensity of the BSE signal depends on the mean atomic number of the target, ESEM-BSE images allow distinguishing between relicts of brines (NaCl rich structures with brighter signal) from brine solution (darker signal). For example, a dark area in Fig. 6 indicates the presence of a brine solution, and as the RH increases, so does the size of the dark area and therefore the amount of brine. When RH reaches 77 %, partial dissolution of the nano-porous structure occurs (Fig. 6d), as evidenced by the extensive dark area and larger dark spots. Another series of ESEM images (Fig. 7a–c) show the dynamics of pore brine in the presence of a cyanobacteria cell during a dehydration cycle at decreasing RH (from 76 % to 30 %). At high RH, pore brine is observed around the cyanobacteria cells aggregate and filling small cracks in the halite (Fig. 7a). The cells aggregate is turgid due to the presence of water. Pore brine progressively disappears around the cyanobacteria cells aggregate and in the narrow cracks, with decreasing RH

BGD
9, 3071–3098, 2012

up to 70 % (Fig. 7b). After a total time of 98 min and when RH decreases to 30 %, the cyanobacterial cells aggregate shows evidence of shrinkage from water loss, although small pockets of brine (dark spots) can still be observed around the cells aggregate (white arrows in Fig. 7c). The composition of this brine (NaCl and H_2O) was confirmed by EDS microanalysis. This experiment demonstrates that even at RH of 30 % a small quantity of brine can be retained by the halite.

3.4 Modeling of capillary condensation process

The DRH of a mineral phase inside a rock, and the evaporation rates of interstitial liquid solutions, not only depend on the temperature and salt concentration of the solution but also on the small pore-space distribution of the rock (Benavente et al., 2003). We modeled the equilibrium RH (RH_{eq}) of a saturated NaCl solution as a function of pore-space using a derivation of the Kelvin model (Benavente et al., 2003). This model predicts that liquid water will nucleate from the vapor phase inside a given pore when $RH > RH_{eq}$. Assuming that the liquid solution is saturated with the host salt, the model predicts a RH_{eq} inside halite between 29 % and 75 % for a pore-radius between 1 and 100 nanometers, respectively (Fig. 8). The range of RH that allows for liquid water condensation in nanometer-size pores overlaps the RH range at which we observed liquid water condensation inside the pinnacles, suggesting that the halite nano-porous phase could indeed be responsible for water vapor condensation at RH significantly lover then DRH. Once liquid water nucleates in the smallest pores, the model predicts a positive feedback mechanism for liquid water condensation as long as $RH > RH_{eq}$, until equilibrium is reached at RH = 75 %, which is the RH_{eq} of a saturated solution of NaCl. This is in fact observed inside the pinnacles at the onset of wet stage, when RH and conductivity inside the pinnacles increase abruptly to 75 % and saturation levels, respectively. Evaporation rates of brines are much lower than that of pure water because the dissolved salt lowers the vapor pressure of the solution (Desbois et al., 2008). Hence brines will tend to stay in the liquid phase longer than pure water. Additionally, our derivation of the Kelvin model indicates that in order to evaporate the

BGD
9, 3071–3098, 2012

pore-water brine in the smaller pores of the halite pinnacles RH inside the halite must fall below 30–40 %, which occurs rarely in the natural environment. Hence, the pinnacle interior is extremely efficient at condensing liquid water from atmospheric vapor even at low RH (~ 51.8 %), and also very efficient at protecting this liquid water from evaporation until RH falls to very low values (~ 41.8 %). Additionally, the outer, non-colonized layer of the halite, with an average pore radius of 42.6 nm and as little as 9.4 % total porosity, is likely to act as a diffusion-limiting layer preventing water vapor exchange with the atmosphere.

4 Conclusions

Endolithic communities inside halite pinnacles in the Atacama Desert take advantage of the moist conditions that are created by the halite substrate in the absence of rain, fog or dew. The tendency of the halite to condense and retain liquid water is enhanced by the presence of a nano-porous phase between larger, massive halite crystals, which are intimately associated to the endolithic communities. This nano-porous face triggers the condensation of liquid water at RH significantly lower than the established DRH point of halite (i.e. 50–55 % instead of 75 %), and also help retain liquid water against evaporation down to RH of 30 %. While halite endoliths must still be adapted to stress conditions inside the pinnacles (i.e. low water activity due to high salinity), these observations show that hygroscopic salts such as halite become oasis for life in extremely dry environments, when all other survival strategies fail.

Our findings have implications for the habitability of extremely dry environments, as they suggest that salts with properties similar to halite could be the preferred habitat for life close to the dry limit on Earth and elsewhere (Davila et al., 2010). It is particularly tempting to speculate that the chloride-bearing evaporites recently identified on Mars (Osterloo et al., 2008), may have been the last, and therefore most recently inhabited substrate, as this planet transitioned from relatively wet to extremely dry conditions.

BGD
9, 3071–3098, 2012

Supplementary material related to this article is available online at: http://www.biogeosciences-discuss.net/9/3071/2012/ bgd-9-3071-2012-supplement.pdf.

Acknowledgements. The authors thank S. Valea and B. Camara for help with installing the microweather station and K. Wierzchos for data treatment. We are grateful to J. A. Nienow for initial idea of electrical conductivity measurements and B. Gómez Silva for logistic support in Yungay. We also acknowledge L. F. Pinto and T. Carnota for technical assistance and A. Burton for reviewing the English. J. W., C. A. and A. F. D. were supported by grant CGL2010-16004 and C. A. by grant CTM2009-12838-C04-03 from the Spanish Ministry of Science and Innovation, and A. F. D. and J. W. were supported by grant NNX12AD61G of the NASA Exobiology program.

References

Ascaso, C., Wierzchos, J., Souza-Egipsy, V., de los Ríos, A., and Rodrigues, J. D.: In situ evaluation of the biodeteriorating action of microorganisms and the effects of biocides on carbonate rock of the Jeronimos Monastery (Lisbon), Int. Biodeter. Biodegr., 49, 1–12, 2002.

Azúa-Bustos, A., González-Silva, C., Mancilla, R. A., Salas, L., Gómez-Silva, B., McKay, C. P., and Vicuña, R.: Hypolithic Cyanobacteria supported mainly by fog in the coastal range of the Atacama Desert, Microb. Ecol., 61, 568–581, 2011.

Benavente, D., García del Cura, M. A., and Ordóñez, S.: Salt influence on evaporation from porous building rocks, Constr. Build. Mater., 17, 113–122, 2003.

Büdel, B., Bendix, J., Bicker, F. R., and Green, A. T. G.: Dewfall as a water source frequently activates the endolithic cyanobacterial communities in the granites of Taylor Valley, Antarctica, J. Phycol., 44, 1415–1424, 2008.

Connon, S. A., Lester, E. D., Shafaat, H. S., Obenhuber, D. C., and Ponce, A.: Bacterial diversity in hyperarid Atacama desert soils, J. Geophys. Res.-Biogeo., 112, G04S17, doi:10.1029/2006JG000311, 2007.

Davila, A. F., Gómez-Silva, B., de los Ríos, A., Ascaso, C., Olivares, H., McKay, C. P., and Wierzchos, J.: Facilitation of endolithic microbial survival in the hyperarid core of the Atacama Desert by mineral deliquescence, J. Geophys. Res.-Biogeo., 113, G01028, doi:10.1029/2007jg000561, 2008.

Davila, A. F., Duport, L. G., Melchiorri, R., Janchen, J., Valea, S., de los Ríos, A., Fairen, A. G., Mohlmann, D., McKay, C. P., Ascaso, C., and Wierzchos, J.: Hygroscopic salts and the potential for life on Mars, Astrobiology, 10, 617–628, 2010.

Desbois, G., Urai, J. L., Burkhardt, C., Drury, M. R., Hayles, M., and Humbel, B.: Cryogenic vitrification and 3D serial sectioning using high resolution cryo-FIB SEM technology for brine-filled grain boundaries in halite: first results, Geofluids, 8, 60–72, 2008.

Desbois, G., Urai, J. L., Kukla, P. A., Wollenberg, U., Pérez-Willard, F., Radí, Z., and Riholm, S.: Distribution of brine in grain boundaries during static recrystallization in wet, synthetic halite: insight from broad ion beam sectioning and SEM observation at cryogenic temperature, Contrib. Mineral. Petr., 163, 19–31, 2012.

Ebert, M.: Environmental scanning electron microscopy as a new technique to determine the hygroscopic behaviour of individual aerosol particles, Atmos. Environ., 36, 5909–5916, 2002.

Ewing, S. A., Yang, W., DePaolo, D. J., Michalski, G., Kendall, C., Stewart, B. W., Thiemens, M., and Amundson, R.: Non-biological fractionation of stable Ca isotopes in soils of the Atacama Desert, Chile, Geochim. Cosmochim. Ac., 72, 1096–1110, 2008.

Friedmann, E. I.: Adaptations of cryptoendolithic lichens in the Antarctic Dry Valleys, Origins Life Evol. B, 12, 320, 1982.

Golubic, S., Friedmann, I., and Schneider, J.: The lithobiontic ecological niche, with special reference to microorganisms, J. Sediment. Petrol., 51, 475–478, 1981.

Hajnos, M., Lipiec, J., Swieboda, R., Sokolowska, Z., and Witkowska-Walczak, B.: Complete characterization of pore size distribution of tilled and orchard soil using water retention curve, mercury porosimetry, nitrogen adsorption, and water desorption methods, Geoderma, 135, 307–314, 2006.

Henschel, J. R. and Seely, M. K.: Ecophysiology of atmospheric moisture in the Namib Desert, Atmos. Res., 87, 362–368, 2008.

Kidron, G.: Microclimate control upon sand microbiotic crusts, Western Negev Desert, Israel, Geomorphology, 36, 1–18, 2000.

Koop, T., Kapilashrami, A., Molina, L. T., and Molina, M. J.: Phase transitions of sea-salt/water mixtures at low temperatures: implications for ozone chemistry in the polar marine boundary layer, J. Geophys. Res.-Atmos., 105, 26393–26402, 2000.

Kuhlman, K. R., Venkat, P., La Duc, M. T., Kuhlman, G. M., and McKay, C. P.: Evidence of a microbial community associated with rock varnish at Yungay, Atacama Desert, Chile, J.

BGD

9, 3071–3098, 2012

Geophys. Res., 113, G04022, doi:10.1029/2007jg000677, 2008.
Lange, O. L., Meyer, A., and Büdel, B.: Net photosynthesis activation of a desiccated cyanobacterium without liquid water in high air humidity alone. Experiments with Microcoleus Sociatus isolated from a desert soil crust, Funct. Ecol., 8, 52–57, 1994.
Lester, E. D., Satomi, M., and Ponce, A.: Microflora of extreme arid Atacama Desert soils, Soil Biol. Biochem., 39, 704–708, 2007.
McKay, C. P., Friedmann, E. I., Gómez-Silva, B., Cáceres-Villanueva, L., and Andersen, D. T.: Temperature and moisture conditions for life in the of observations including the El Niño of 1997–1998, Astrobiology, 3, 393–406, 2003.
Navarro-González, R., Rainey, F. A., Molina, P., Bagaley, D. R., Hollen, B. J., De La Rosa, J., Small, A. M., Quinn, R. C., Grunthaner, F. J., Cáceres, L., Gómez-Silva, B., and McKay, C. P.: Mars-like soils in the Atacama Desert, Chile, and the dry limit of microbial life, Science, 302, 1018–1021, 2003.
Nienow, J. A.: Extremophiles: dry environments (including Cryptoendoliths), in: Encyclopedia of Microbiology, Elsevier, Oxford, 159–173, 2009.
Osterloo, M. M., Hamilton, V. E., Bandfield, J. L., Glotch, T. D., Baldridge, A. M., Christensen, P. R., Tornabene, L. L., and Anderson, F. S.: Chloride-bearing materials in the southern highlands of Mars, Science, 319, 1651–1654, 2008.
Palmer, R. J. and Friedmann, E. I.: Water relations, thallus structure and photosynthesis in Negev Desert lichens, New Phytol., 116, 597–603, 1990a.
Palmer, R. J. and Friedmann, E. I.: Water relations and photosynthesis in the cryptoendolithic microbial habitat of hot and cold deserts, Microb. Ecol., 19, 111–118, 1990b.
Pueyo, J. J., Chong, G., and Jensen, A.: Neogene evaporites in desert volcanic environments: Atacama Desert, Northern Chile, Sedimentology, 48, 1411–1431, 2001.
de los Ríos, A., Valea, S., Ascaso, C., Davila, A., Kastovsky, J., McKay, C. P., Gómez-Silva, B., and Wierzchos, J.: Comparative analysis of the microbial communities inhabiting halite evaporites of the Atacama Desert, Int. Microbiol., 13, 79–89, 2010.
Schenk, O., Urai, J. L., and Piazolo, S.: Structure of grain boundaries in wet, synthetic polycrystalline, statically recrystallizing halite – evidence from cryo-SEM observations, Geofluids, 6, 93–104, 2006.
Souza-Egipsy, V., Ascaso, C., and Sancho, L. G.: Water distribution within terricolous lichens revealed by scanning electron microscopy and its relevance in soil crust ecology, Mycol. Res., 106, 1367–1374, 2002.

BGD
9, 3071–3098, 2012

Tang, I. N. and Munkelwitz, H. R.: Composition and temperature dependence of the deliquescence properties of hygroscopic aerosols, Atmos. Environ. A-Gen., 27, 467–473, 1993.

Tang, I. N., Tridico, A. C., and Fung, K. H.: Thermodynamic and optical properties of sea salt aerosols, J. Geophys. Res.-Atmos., 102, 23269–23275, 1997.

Warren-Rhodes, K. A., Rhodes, K. L., Pointing, S. B., Ewing, S. A., Lacap, D. C., Gómez-Silva, B., Amundson, R., Friedmann, E. I., and McKay, C. P.: Hypolithic cyanobacteria, dry limit of photosynthesis, and microbial ecology in the hyperarid Atacama Desert, Microb. Ecol., 52, 389–398, 2006.

Wierzchos, J., Ascaso, C., and McKay, C. P.: Endolithic cyanobacteria in halite rocks from the hyperarid core of the Atacama Desert, Astrobiology, 6, 415–422, 2006.

Wierzchos, J., Cámara, B., de los Ríos, A., Dávila, A. F., Sánchez Almazo, I. M., Artieda, O., Wierzchos, K., Gómez-Silva, B., McKay, C., and Ascaso, C.: Microbial colonization of Ca-sulfate crusts in the hyperarid core of the Atacama Desert: implications for the search for life on Mars, Geobiology, 9, 44–60, 2011.

BGD

9, 3071–3098, 2012

Novel water source for endolithic life in the hyperarid core of the Atacama Desert

J. Wierzchos et al.

Table 1. Mercury intrusion porosimetry data.

	Superficial zone	Colonized zone
Total intrusion volume[a] [$ml\,g^{-1}$]	0.0489 $\sigma = 0.00$	0.1164 $\sigma = 0.00$
Total pore area [$m^2\,g^{-1}$]	2.37 $\sigma = 0.77$	1.78 $\sigma = 0.63$
Median pore radius (vol.) [nm]	3831.07 $\sigma = 1529$	6942.22 $\sigma = 1159$
Median pore radius (area) [nm]	2.56 $\sigma = 0.74$	3.17 $\sigma = 1.42$
Average pore diameter/2 = radius[b] ($4V/A$) [nm]	42.65 $\sigma = 9.15$	153.10 $\sigma = 87.08$
Bulk density[c] [$g\,cm^{-3}$]	1.94 $\sigma = 0.06$	1.72 $\sigma = 0.04$
Total porosity[d] [%]	9.40 $\sigma = 2.14$	19.84 $\sigma = 1.84$
Total intrusion volume [$ml\,g^{-1}$] for pores < 100 nm	0.0057	0.0067
Fraction in [%] of total porosity for pores < 100 nm	11.73	5.76

[a] Volume of Hg introduced for maximum (413 MPa) pressure.

[b] The average pore diameter ($4V/A$) obtained by assuming that pore volume ($V = \pi d^2 L/4$) is divided by the pore area ($A = \pi d L$), the average pore diameter (d) is equal to $4V/A$.

[c] Bulk density at 0.0036 MPa pressure.

[d] Total porosity – the ratio of pore volume to apparent volume of the sample (calculated on the basis of the bulk density) expressed as a percentage.

BGD
9, 3071–3098, 2012

BGD
9, 3071–3098, 2012

Novel water source for endolithic life in the hyperarid core of the Atacama Desert

J. Wierzchos et al.

Title Page
Abstract | Introduction
Conclusions | References
Tables | Figures
◀| |▶
◀ ▶
Back | Close
Full Screen / Esc
Printer-friendly Version
Interactive Discussion

Table 2. Micro-environmental data measured simultaneously outside and inside halite pinnacles in the Yungay region.

Variable	Halite exterior	Halite interior
Mean annual RH, %	34.75	54.74
Maximum annual RH, %	74.20	86.10
Minimum annual RH, %	2.90	2.20
σ or RH measurements	19.50	27.99
Mean annual T, °C	18.03	17.94
Maximum annual T, °C	45.06	51.00
Minimum annual T, °C	–6.17	–9.47
σ or T measurements	11.24	13.76
Annual wet events[a], h yr^{-1}	0	5362
Annual wet events[b], h yr^{-1}	0	3909

[a] for $EC_{In} > 0.0006$;
[b] for $RH_{In} > 75\,\%$

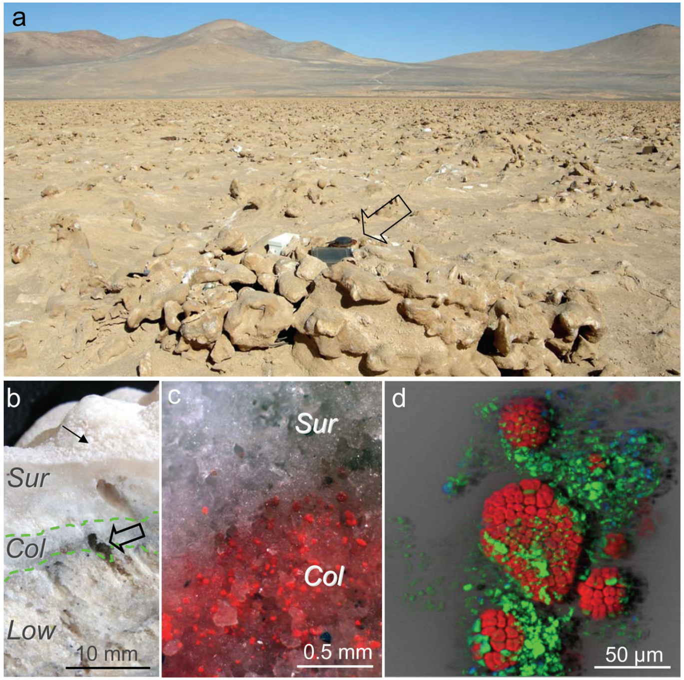

Fig. 1. Halite pinnacles and their endolithic microbial community in the Yungay region of the Atacama Desert. **(a)** Group of halite pinnacles with the microweather station in the foreground (open arrow). **(b)** Fractured halite pinnacle with a non-colonized outer layer (Sur), colonized intermediate zone (Col) with larger pores (open arrow), and a non-colonized inner layer (Low). Note the halite efflorescence on the pinnacle surface (black arrow), which indicates recent brine evaporation. **(c)** Fluorescence microscopy (FM) reveals the sharp boundary between the non-colonized outer layer, and the colonized zone (red autofluorescence of cyanobacterial aggregates). **(d)** In situ 3-D FM-SIM image of cyanobacterial aggregates (red autofluorescence signal), and associated heterotrophic bacteria and archaea (SYBR Green stained DNA structures green signal).

BGD
9, 3071–3098, 2012

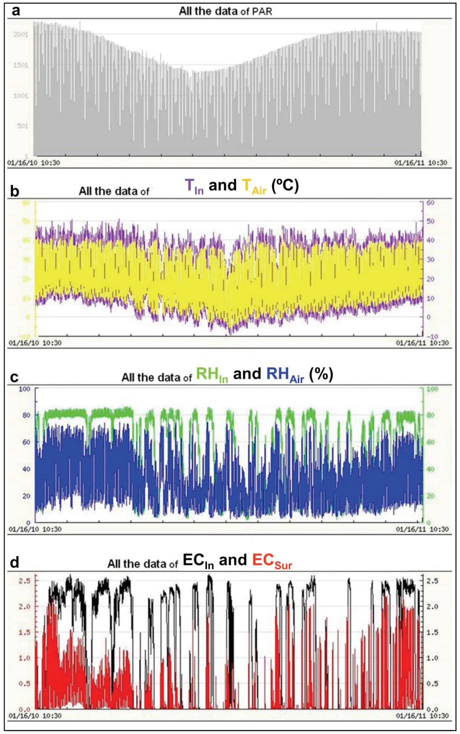

Fig. 2. Micro-environmental data collected over one year inside and outside halite pinnacles in the Yungay region. **(a)** Photosynthetic active radiation (PAR). **(b)** Temperature inside the pinnacle (T_{In}, purple line) and atmospheric temperature (T_{Air}, yellow line). Note the higher temperature amplitudes inside the pinnacle. **(c)** Relative humidity inside the pinnacle ($\mathrm{RH_{In}}$, green line) and air relative humidity ($\mathrm{RH_{Air}}$, blue line). Note the long periods when $\mathrm{RH_{In}}$ was above 75 % (deliquescence relative humidity), while $\mathrm{RH_{Air}}$ never exceeded 75 %. **(d)** Electrical conductivity inside the halite pinnacle ($\mathrm{EC_{In}}$, black line) and surface electrical conductivity ($\mathrm{EC_{Sur}}$, red line). Note the long periods when $\mathrm{EC_{In}}$ and also $\mathrm{EC_{Sur}}$ values were above 0, indicating the presence of liquid water.

BGD
9, 3071–3098, 2012

Novel water source for endolithic life in the hyperarid core of the Atacama Desert

J. Wierzchos et al.

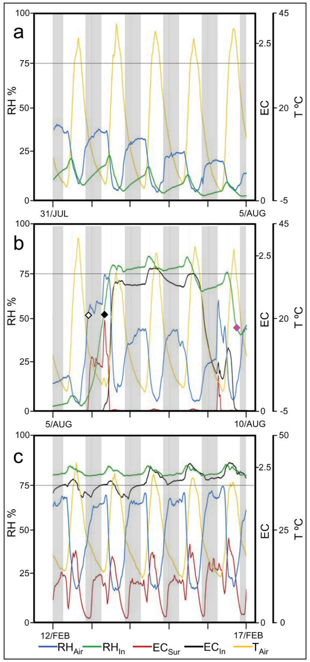

Fig. 3. Moisture conditions inside and outside the halite pinnacles. Grey vertical stripes indicate night time dark hours. **(a)** Dry stage when RH_{Air} and RH_{In} fall below 40 % and 25 %, respectively, and EC sensors record null values. **(b)** Short wet event. Water condensation occurs first on the halite surface (white diamond), and is followed several hours later by capillary condensation in the colonization zone (black diamond); the pinnacle falls back to the dry stage after four days of wet internal conditions (pink diamond). **(c)** Portion of a 40-day-long wet stage, when RH_{In} is continuously above 75 %. Concurrently, RH_{Air} oscillates between 17–19 % (afternoons) and 70–74 % (nights and dawn). Positive EC values indicate liquid water inside the pinnacles and on their surface. Note that the maximum EC_{Sur} value was observed between 01:00 and 03:00 p.m., at lowest RH_{Air} and highest daily T_{Air}. RH_{Air} = atmospheric RH; T_{Air} = atmospheric T; RH_{In} = RH in halite interior; EC_{Sur} = conductivity on halite surface; EC_{In} = conductivity in halite interior.

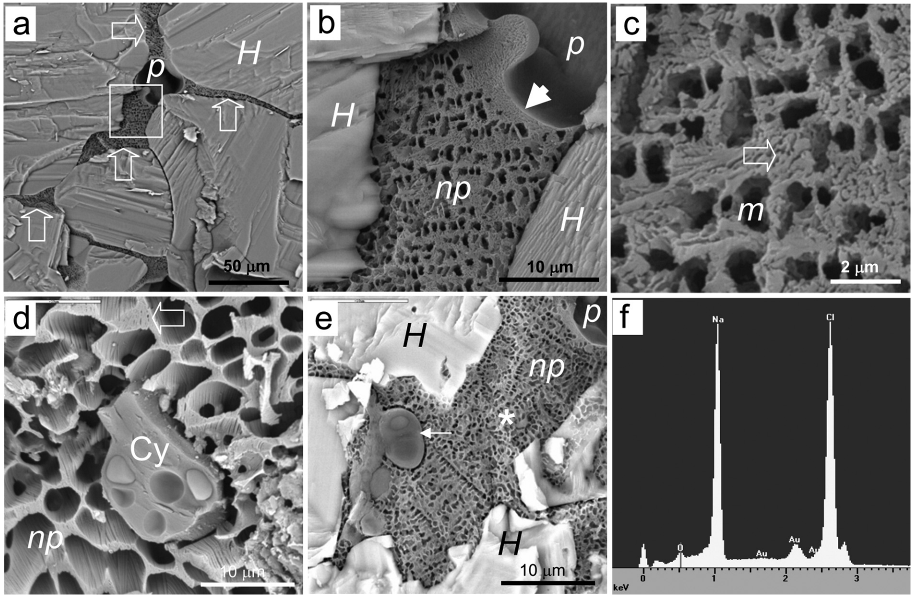

Fig. 4. SEM images of the endolithic habitat inside the pinnacles. **(a)** LT-SEM image showing pore spaces between halite crystals (*H*) and a nano-porous halite phase filling the grain boundary (open arrows) and large pore (*p*). Inset shown in **(b)**, Detail image of the nano-porous halite phase (np) with a smooth surfaced (head arrow) in contact with a pore (*p*). **(c)** High magnification LT-SEM image of the nano-porous phase revealing micro-pores (*m*, 0.5–1.5 µm diameter) and nano-pores (< 100 nm, open arrow). Images **(a–c)** are dry samples previously equilibrated at 20 % RH. **(d)** LT-SEM image of cyanobacterial cells aggregate (Cy) embedded in the nano-porous halite phase of a dry sample equilibrated at 40 % RH. Note the capillary shape of the nano-pores (open arrow). **(e)** LT-SEM image of cyanobacterial cells (arrow) embedded in the nano-porous phase in a sample equilibrated at 75 % RH. **(f)** Energy dispersive spectroscopy of the nano-porous phase (asterisk in **e**) reveals Na and Cl as main elements.

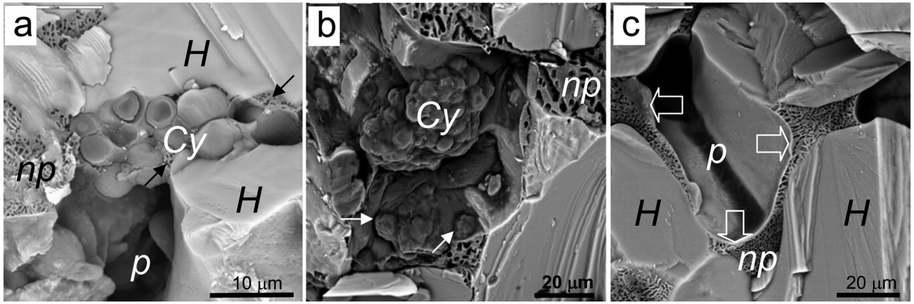

Fig. 5. LT-SEM images of the endolithic aggregates, and the nano-porous halite phase, inside a pinnacle. **(a)** Endolithic cyanobacterial (Cy) aggregates attached to massive halite crystals (*H*). Also shown are the nano-porous phase (np), and an empty pore (*p*); black arrows point to np among the microbial cells. **(b)** Cyanobacterial aggregate and heterotrophic bacterial aggregates (white arrows) embedded in the nano-porous phase. **(c)** Larger halite crystals surrounded by the nano-porous phase.

BGD
9, 3071–3098, 2012

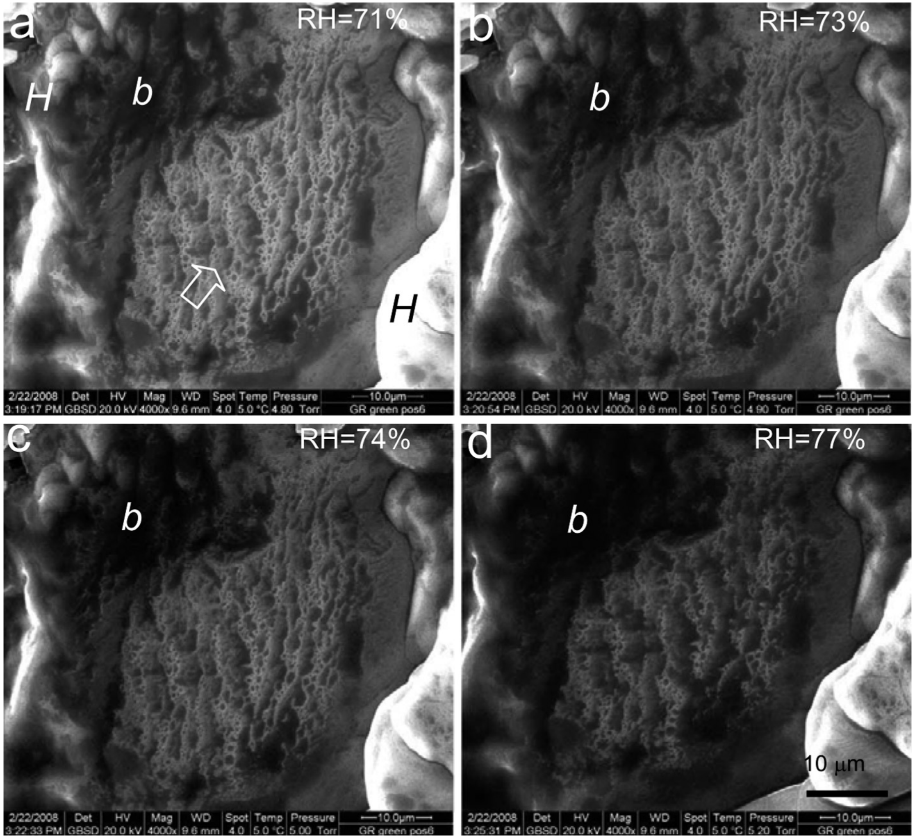

Fig. 6. Sequence of ESEM-BSE images showing the nano-porous phase (open arrow in **(a)** and central part of following images) among larger halite crystals (*H*) in samples equilibrated inside the ESEM chamber at RH between 71 % and 77 %; (*b*) = brine solution.

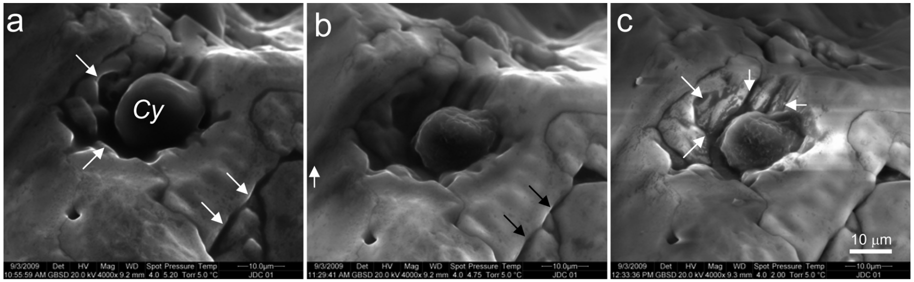

Fig. 7. ESEM in situ imaging of halite dehydration from RH = 76 % **(a)**; RH = 70 % **(b)**; and RH = 30 % **(c)**; Cy, cyanobacterial cells aggregate; white arrows point to brine solution; black arrows point to partially evaporated brine in narrow fissure. Note how the cyanobacterial aggregate shrinks with decreasing RH and brine evaporation. Scale bar applies to all images.

BGD

9, 3071–3098, 2012

Title Page
Abstract | Introduction
Conclusions | References
Tables | Figures
◀| |▶
◀ ▶
Back | Close
Full Screen / Esc
Printer-friendly Version
Interactive Discussion

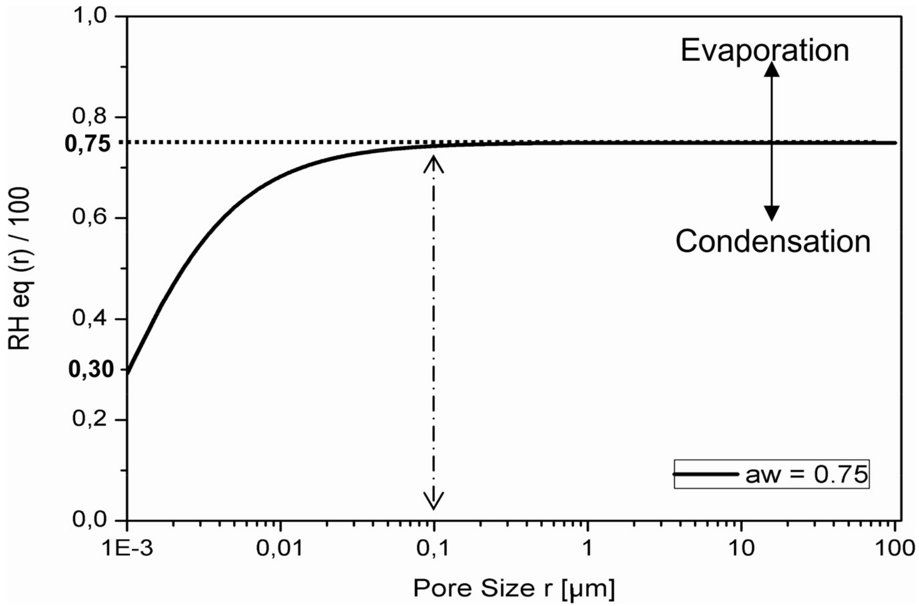

Fig. 8. Theoretical water evaporation/condensation equilibrium in halite. The model estimates the equilibrium relative humidity (RH_{eq}) of a NaCl saturated solution as a function or pore radius (Benavente et al., 2003). See Supplement for more details.

BGD
9, 3071–3098, 2012